Computer Modeling in Engineering & Sciences

Tech Science Press

DOI: 10.32604/cmes.2023.025769

check for updates

ARTICLE

Study of Fractional Order Dynamical System of Viral Infection Disease under Piecewise Derivative

Kamal Shah[1,2], Hafsa Naz[2], Thabet Abdeljawad[1,3,*] and Bahaaeldin Abdalla[1]

[1]Department of Mathematics and Sciences, Prince Sultan University, P.O. Box 66833, Riyadh, 11586, Saudi Arabia

[2]Department of Mathematics, University of Malakand, Chakdara Dir(L), Khyber Pakhtunkhwa, 18000, Pakistan

[3]Department of Medical Research, China Medical University, Taichung, 40402, Taiwan

*Corresponding Author: Thabet Abdeljawad. Email: tabdeljawad@psu.edu.sa

Received: 29 July 2022 Accepted: 07 September 2022

ABSTRACT

This research aims to understand the fractional order dynamics of the deadly Nipah virus (NiV) disease. We focus on using piecewise derivatives in the context of classical and singular kernels of power operators in the Caputo sense to investigate the crossover behavior of the considered dynamical system. We establish some qualitative results about the existence and uniqueness of the solution to the proposed problem. By utilizing the Newtonian polynomials interpolation technique, we recall a powerful algorithm to interpret the numerical findings for the aforesaid model. Here, we remark that the said viral infection is caused by an *RNA* type virus which can transmit from animals and also from an infected person to person. Fruits bats which are also known as flying foxes are one of the sources of transmission of NiV disease. Here in this work, we investigate its transmission mechanism through some new concepts of fractional calculus for further analysis and prediction. We present the approximate results for different compartments using different fractional orders. By using the piecewise derivative concept, we detect the crossover or multi-steps behavior in the transmission dynamics of the mentioned disease. Therefore, the considered form of the derivative is used to deal with problems exhibiting crossover behaviors.

KEYWORDS

NiV disease; fractional calculus; piecewise derivative; qualitative results; newton polynomial; RNA virus

1 Introduction

From ancient times, viral diseases have remained a great threat to human as well as animal life on this globe. The said infections have caused millions of death in the past. Sometimes these infections have given birth to various terrible outbreaks in which millions of people lost their lives. For instance, viral infections like swine flu, MERS, bird flu, Nipah, and Henipa have triggered global public health disasters in the last many decades [1]. These infections have reappeared after some period of time and spread dramatically in most parts of the world. During their transmission, millions of people have died (see [2,3]). NiV disease is a highly contagious viral disease and can transmit among animals and humans. NiV infection causes encephalitis (brain swelling), which can vary from severe chronic sickness to even death. The said virus was identified for the first time in the town of Malaysia Nipah in

1998. Therefore, this virus has been named NiV. It was initially identified in a patient in the said town of Malaysia. From September 1998 to May 1999, it was initially identified in a massive epidemic of 276 cases in Peninsular Malaysia and Singapore [4]. Migratory fruit bats have been reported as natural reservoirs of this disease. Bats that are infected transmit viruses through their wastes and mucus, such as spitting, urinating, and reproductive cells. Hence, they are asymptomatic carriers of the disease [5,6]. The NIV is extremely infectious in pigs and transmitted through coughing. Direct contact with infected pigs has been found to be the primary mechanism of transfer in individuals when it was initially detected in a massive epidemic in Malaysia in 1999 (see [7]). More than eighty percent of people during the 1998 to 1999 outbreaks were belonging to the pigs' farmers' community or were exposed to pigs (see [8]).

The awareness of NiV transmission has made tremendous progress over the last two decades, especially in ways to investigate and study human Nipah microbial infections. Also, WHO declared it as one of the most dangerous and highly contagious diseases in 2015. Diagnostic equipment has been invented in the context of the Malaysian pandemic which is helping us to detect cases much more easily. Two NiV epidemics arose in India and Bangladesh in 2001 (see detail [9]). After outbreaks in the Philippines in 2014 as well as in Kerala India in 2018, the geographic range of human infections of the NiV virus has continued to expand. NiV is a disease that can be passed from person to person, but no cases have been reported in Malaysia or Singapore in this context. Incidents of humans to humans and animals to humans have been reported in Bangladesh, the Philippines, and India. More research on the dynamics of NiV transmission, however, is required. Clear symptoms of NiV illness include fever, memory problems, migraines, dysentery, asthma, chest tightness, extreme weakness, and tremors [10]. Approximately 10% of the total number of Nipah-infected people transmit the virus to others. The most efficient technique to prevent the infection from spreading is quarantine. The majority of viral infections behave in an unanticipated manner. However, there are a number of elements that contribute to a viral disease's becoming a pandemic [11]. In the case of the said disease, the primary reservoir, genetic mutations, infectious transmitters, speed of transmission, and overflow from animal sources are some of the crucial components that should be addressed with it and comprehended in order to control the next pandemic outbreak [12]. Recently some updated work has been published on NiV disease. For example, authors [13] have analyzed the immunology of the virus. Similarly on new analysis and information about the said disease, authors have published good results in [14,15] recently.

Here, we demonstrate that mathematical models are essential tools for understanding how to effectively investigate the dynamics of transmissions and treatment of these infections. We refer to the importance of the mathematical model of the book for the reader in [16]. The literature on NiV contains a wide diversity of research. A few researchers have worked on the medical trial of NIV disease (see [17]). The authors have explained the characteristic symptoms of the disease encephalitis patients among Malaysian pigs and its psychological effect on human life (we refer to [18]). Further, some researchers worked on controlling of the disease in the community (see [19]). Some authors have worked on clinical trials. For instance, authors [20] have investigated the clinical features of NiV encephalitis among pig farmers in Malaysia. In the same line, authors [21] have studied differences in epidemiologic and clinical features of Nipah virus encephalitis between the Malaysian and Bangladesh outbreaks. Additionally, authors [22] have analyzed the clinical presentation of NiV disease in Bangladesh. Biswas established a mathematical model consisting of ordinary differential equations for the transmission of the NiV disease. The said model has been solved numerically by the said author. Further, some authors investigated the nature of the infection using an optimal control method [23].

So far, ordinary derivatives have been used as powerful tools to study the dynamical behavior of real-world problems. Since most of the dynamical problems suffer from abrupt or sudden changes in their state of rest or motions and hence show multi-behavior which is known as crossover behavior. It has been investigated that the said behavior cannot be explained by the concept of traditional calculus properly. Also, ordinary fractional order derivatives involving exponential, Mittag-Leffler, and power law kernel do not explain these terms significantly. It is because many real-world models exhibit crossover phenomena that are difficult to describe using traditional fractional order derivatives. For instance, earthquakes, pendulum motion, and contemporary economic fluctuations in less developed nations, experience rapid shifts in their state of dynamics. Instead of utilizing continuous derivatives, piecewise derivatives have been proved an ideal way to show this crossover phenomenon. In this context, the mentioned derivative's key characteristics have recently been examined in [24]. The authors have defined the classical and global piecewise derivatives, as well as several examples. Here it should be kept in mind that traditional fractional order derivative has been increasingly used in mathematical models of various infectious diseases like COVID-19. A mathematical model of COVID-19 using fractional order derivative has been investigated in [25]. Moreover, some mathematical models under the fractional order derivatives have been investigated in [26]. In the same line, the author has also studied a model of COVID-19 using the concept of fractional calculus. Authors [27] have studied attractors of chaotic dynamical systems with fractal-fractional operators. In the same fashion, authors [28] have established a fractional order model for the investigation of COVID-19. Furthermore, authors [29] have investigated a fractional order susceptible, infected, and recovered epidemic model of childhood disease numerically. Authors [30] have developed and analyzed a mathematical model for the dynamics of COVID-19 with re-infection. In the same line, authors [31] have considered the fractional order predator-prey model with the harvesting rate. Keeping the importance of fractional calculus, authors [32] have investable transmission dynamics of Nipah virus disease under Caputo fractional derivative.

2 Formulation of NiV Model

Inspired by the importance of fractional calculus, we considered the integer order model of NiV which has been studied under some new concept of fractional order derivative. Authors [33] have presented a novel NiV disease model under traditional order derivative as presented in Fig. 1 and described as

$$\begin{aligned}
\frac{d\mathbf{S}}{dt} &= \Pi - \frac{\beta \mathbf{I}\mathbf{S}}{\mathbf{N}} - \mu \mathbf{S} \\
\frac{d\mathbf{E}}{dt} &= \frac{\beta \mathbf{I}\mathbf{S}}{\mathbf{N}} - \Phi \mathbf{E} - \mu \mathbf{E} \\
\frac{d\mathbf{I}}{dt} &= \Phi \mathbf{E} + \eta \mathbf{T} - (\Upsilon + \varepsilon_1 + \rho + \mu)\, \mathbf{I} \\
\frac{d\mathbf{T}}{dt} &= \Upsilon \mathbf{I} - (a + \eta + \theta\rho + \varepsilon_2 + \mu)\, \mathbf{T} \\
\frac{d\mathbf{R}}{dt} &= a\mathbf{T} + \varepsilon_1 \mathbf{I} + \varepsilon_2 \mathbf{T} - \mu \mathbf{R},
\end{aligned} \tag{1}$$

where various compartments, parameters and variables involved in the model are explained in the Table 1. Here, the total population of the community at time t is $\mathbf{N}$, which we divide into five compartments including susceptible, exposed, infected, treated, and recovered classes respectively. Let the susceptible class $\mathbf{S}$ population be recruited at the rate Π, and diminished by the class who gets

an infection and hence follows contact with an infected class at a rate $\frac{\beta \mathbf{I}}{\mathbf{N}}$. Due to the natural death rate, the susceptible population further decays by the amount $\mu\mathbf{S}$. In the same fashion, the class **E** is generated by the susceptible class when it comes in contact with infected people at the rate $\frac{\beta \mathbf{I}}{\mathbf{N}}$. The exposed population is further reduced by the infection rate Φ and a natural death rate μ. Due to infection rate Φ in the exposed class and individuals who get an infection in the treating class at a rate η, the population of the infected class is generated as $\Phi\mathbf{E} + \eta\mathbf{T}$. The population of the infected class is reduced by the natural death rate $\boldsymbol{\mu}$, treatment rate Υ, and natural recovery rates in infected and treatment groups at rates ε_1 and ρ death rate of infection respectively. Furthermore, the treated class is generated from the infected class with rate Υ and reduced by rates a, η, $\theta\rho$, ε_2, μ, respectively. The last recovered class is generated at the rate a, ε_1, and ε_2 respectively from the treated class, and the population is reduced by natural death rate μ. Hence briefly, we describe the transmission mechanism of the proposed model (1) in the flow chart 1. Authors have investigated NiV disease in [34,35] by using the concept provided in [36].

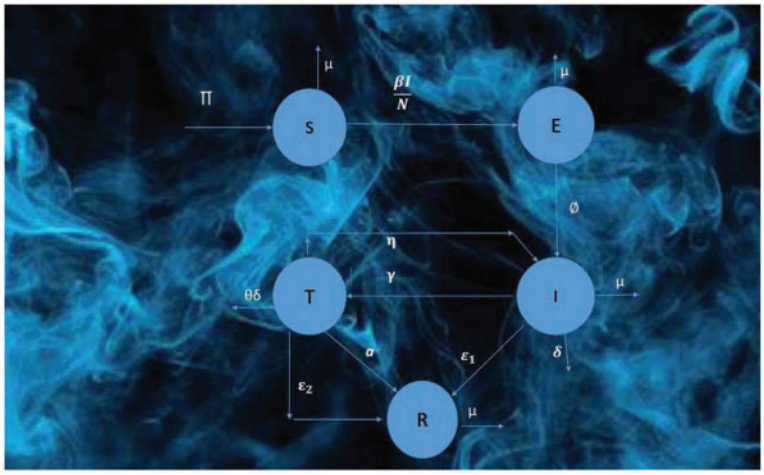

Figure 1: Flow chart of the model (1)

Table 1: The nomenclature and their description of NiV model

Nomenclature	Descriptions
S	Density of susceptible class
E	Density of exposed class
I	Density of infected class
T	Density of treated class
R	Density of recovered class
Π	Birth rate
β	Transmission rate
μ	Rate of natural death
ρ	Rate of death due to infection
Φ	The rate of the exposed population that becomes infected
ε_1 and ε_2	Rate of natural recovery in infected and treatment groups, respectively
a	The rate of recovery as a result of treatment
η	Infection rate
Υ	The rate of progress from **I** to **T**

(Continued)

Table 1 (continued)

Nomenclature	Descriptions
θ	Death rate due to infection of **T**
N	Number of total population

Motivated by the importance of piecewise derivatives, we extend model (1) under the piecewise derivative with fractional order $0 < \alpha \leq 1$ as

$$
\begin{aligned}
{}_{0}^{\mathscr{P}\mathscr{C}}\mathrm{D}_{t}^{\alpha}\mathbf{S}(t) &= \Pi - \frac{\beta \mathbf{IS}}{\mathbf{N}} - \boldsymbol{\mu}\mathbf{S} \\
{}_{0}^{\mathscr{P}\mathscr{C}}\mathrm{D}_{t}^{\alpha}\mathbf{E}(t) &= \frac{\beta \mathbf{IS}}{\mathbf{N}} - \Phi\mathbf{E} - \mu\mathbf{E} \\
{}_{0}^{\mathscr{P}\mathscr{C}}\mathrm{D}_{t}^{\alpha}\mathbf{I}(t) &= \Phi\mathbf{E} + \eta\mathbf{T} - (\Upsilon + \varepsilon_1 + \rho + \mu)\mathbf{I} \\
{}_{0}^{\mathscr{P}\mathscr{C}}\mathrm{D}_{t}^{\alpha}\mathbf{T}(t) &= \Upsilon\mathbf{I} - (a + \eta + \theta\rho + \varepsilon_2 + \mu)\mathbf{T} \\
{}_{0}^{\mathscr{P}\mathscr{C}}\mathscr{D}_{t}^{\alpha}\mathbf{R}(t) &= a\mathbf{T} + \varepsilon_1\mathbf{I} + \varepsilon_2\mathbf{T} - \mu\mathbf{R}
\end{aligned}
\tag{2}
$$

${}_{0}^{\mathscr{P}\mathscr{C}}\mathrm{D}_{t}$ denotes the piecewise classical Caputo derivative in $[0, t_2]$. Inspired by the above discussion, we examine a SEITR-type mathematical model for NiV disease using the piece-wise classical and Caputo fractional order derivatives. Here, we state that the mentioned derivative has been recently utilized for studying various problems, which we refer to as [37,38]. Eventually, the model's formulation is presented. Second, the suggested model includes the fundamental reproduction number as well as disease-free and endemic equilibrium. We develop an attempt at existence theory for the model using the fixed point technique. Before studying dynamical models, it is necessary to examine the existence theory. The existence of real-world problems in the form of mathematical formulation is investigated properly by fixed point theory and other tools of nonlinear functional analysis. For some applications of fixed point theory, we refer to [39,40]. The said fixed point results have used for some problems in [41]. We also use the numerical procedure based on Adam Bashforth method to investigate the numerical analysis of the proposed model at different fractional orders. The mentioned numerical method is a powerful tool. The convergence and stability analysis of the Adams-Bashforth method have been discussed in detail in [42].

3 Basic Results

Here, some basic results are recollected from fractional calculus.

Definition 3.1. [41]. The fractional derivative of **g** of order $0 < \alpha \leq 1$ in Caputo sense is given as

$$
{}_{0}^{\mathscr{C}}D_{t}^{\alpha}\mathbf{g}(t) = \frac{1}{\Gamma(1-\alpha)}\int_{0}^{t}(t-\tau)^{-\alpha}[\mathbf{g}'(\tau)]\,d\tau,
$$

such that right hand side exists.

Definition 3.2. [41]. Fractional integration of **g** w.r.t t of order α is

$$
{}_{0}^{\mathscr{C}}\mathrm{I}_{t}^{\alpha}\mathbf{g}(t) = \frac{1}{\Gamma(\alpha)}\int_{0}^{t}(t-\tau)^{\alpha-1}\mathbf{g}(\tau)\,d\tau,\ \alpha > 0,
$$

such that right hand side exists.

Definition 3.3. [24]. Let $\mathbf{g}$ be differentiable function, then the traditional and arbitrary order piecewise derivative is recalled as

$$ {}_{0}^{\mathscr{P}\mathscr{C}}\mathrm{D}_{\mathrm{t}}^{\alpha}\mathbf{g}\,(\mathrm{t}) = \begin{cases} \mathbf{g}'(\mathrm{t}), & 0 < \mathrm{t} \leq \mathrm{t}_1, \\ {}_{0}^{\mathrm{c}}D_{\mathrm{t}}^{\alpha}\mathbf{g}(\mathrm{t}), & \mathrm{t}_1 < \mathrm{t} \leq \mathrm{t}_2, \end{cases} $$

with $\alpha \in (0, 1]$.

Definition 3.4. Let $\mathbf{g}$ be differentiable, then the classical and fractional order piecewise integration [24] is given as

$$ {}_{0}^{PI}\mathrm{I}_{t}^{\alpha}\mathbf{g}(\mathrm{t}) = \begin{cases} \int_0^{\mathrm{t}} \mathbf{g}(\tau)\mathrm{d}\tau, & 0 < \mathrm{t} \leq \mathrm{t}_1, \\ \frac{1}{\Gamma(\alpha)} \int_{\mathrm{t}_1}^{\mathrm{t}} (\mathrm{t}-\tau)^{r-1}\mathbf{g}\,(\tau)\,\mathrm{d}\,(\tau)\,, & \mathrm{t}_1 < \mathrm{t} \leq \mathrm{t}_2, \end{cases} $$

such that ${}_{0}\mathrm{I}_{\mathrm{t}}^{\alpha}\mathbf{g}(\mathrm{t})$ is Reimann-Liouville integration for $\mathrm{t}_1 < \mathrm{t} \leq \mathrm{t}_2$ and classical integration for $0 < \mathrm{t} \leq \mathrm{t}_1$.

Lemma 3.1. [24] The solution of

$$ {}_{0}^{PC}D_{\mathrm{t}}^{\alpha}\mathbf{g}(\mathrm{t}) = \mathrm{G}(t, \mathbf{g}(\mathrm{t})), 0 < \alpha \leq 1, $$

is given by

$$ \mathbf{g}\,(t) = \begin{cases} \mathbf{g}_0 + \int_0^{t} \mathrm{G}(\tau, \mathbf{g}(\tau))d\tau, 0 < \mathrm{t} \leq \mathrm{t}_1 \\ \mathbf{g}\,(t_1) + \frac{1}{\Gamma(\alpha)} \int_{t_1}^{t} (t-\tau)^{\alpha-1}\mathrm{G}\,(\tau, \mathbf{g}\,(\tau))\,d\,(\tau)\,, \ \mathrm{t}_1 < \mathrm{t} \leq \mathrm{t}_2. \end{cases} $$

4 Qualitative Analysis

Some existence results are derived here. It should be kept in mind that prior to dealing with a dynamical system, existence theory is important to investigate for the prosed problem. As the model is used to estimate the population of humans, it is necessary that all of its parameters and variables for all time t be nonnegative.

Theorem 4.1. [33]. Let $\{\mathbf{S}(0), \mathbf{E}(0), \mathbf{I}(0), \mathbf{T}(0), \mathbf{R}(0) \geq 0\} \in \mathrm{R}_{+}^{5}$. Then, the region of solution is invariant and all solutions are falling in the region representing by

$$ \mathscr{R}_f = \left\{ (\mathbf{S}, \mathbf{E}, \mathbf{I}, \mathbf{T}, \mathbf{R}) \in \mathrm{R}_{+}^{5} : \mathbf{N} \leq \frac{\Pi}{\mu} \right\}. $$

Proof. By adding all equations of model (2), where $\mathbf{N}$ is the total papulation, we have

$$ \begin{aligned} {}_{0}^{\mathscr{C}}D_{\mathrm{t}}^{\alpha}\mathbf{N}(t) &= \Pi - (\mathbf{S} + \mathbf{E} + \mathbf{I} + \mathbf{T} + \mathbf{R})\,\mu - \delta\mathbf{I} - \theta\delta\mathbf{T} \\ &= \Pi - \mathbf{N}\mu - \delta\mathbf{I} - \theta\delta\mathbf{T} \\ &\leq \Pi - \mathbf{N}\mu. \end{aligned} $$

Take Laplace transform of and use $\mathbf{N}(0) = \mathbf{N}_0$, as

$$ \mathscr{L}[{}_{0}^{\mathscr{C}}D_{\mathrm{t}}^{\alpha}\mathbf{N}](t) \leq \mathscr{L}[\Pi - \mathbf{N}\mu] $$

yields after simplification

$$ \mathbf{N}\,(s) \leq \frac{\mathbf{N}_0 s^{\alpha-1}}{s^{\alpha} + \mu} + \frac{\Pi}{s(s^{\alpha} + \mu)}. $$

After evaluating, we have

$$\mathbf{N}(t) \leq \mathbf{N}_0 t\mathscr{E}_{\alpha,1}(-\mu t^{\alpha}) + \frac{\Pi}{\mu}\Big[1 - \mathscr{E}_{\alpha}(-\mu t^{\alpha})\Big], \tag{3}$$

where $\mathscr{E}$ denoted Mittag-Leffler function of one parameter. Further, at $t \to \infty$ in (3), we get

$$\mathbf{N}(t) \leq \frac{\Pi}{\mu}.$$

Also, it is straightforward to show that each compartment is non-negative.

Remark 1. Disease free equilibrium refers to a stable condition in which there is no infection or disease. The said point has been computed in [33] as

$$\varepsilon_0 = (\mathbf{R}^*, \mathbf{I}^*, \mathbf{E}^*, \mathbf{R}^*) = \left(\frac{\Pi}{\mu}, 0, 0, 0\right)$$

and the fundamental threshold number is given by

$$\mathbf{R}_0 = \frac{\beta\Pi\sigma}{\mathbf{N}\mu(\sigma+\mu)(\varepsilon_1+\delta+\mu)}.$$

The said number predicts the transmission dynamics of disease in the community. If $\mathbf{R}_0 < 1$, it indicates a decrease in disease in the community while $\mathbf{R}_0 > 1$ shows a raise in infection in the society. The mentioned number can be computed by using the next generation matrix method which has been discussed in detail in [36].

Some 3D profiles of $\mathbf{R}_0$ against different parameters are given in Fig. 2.

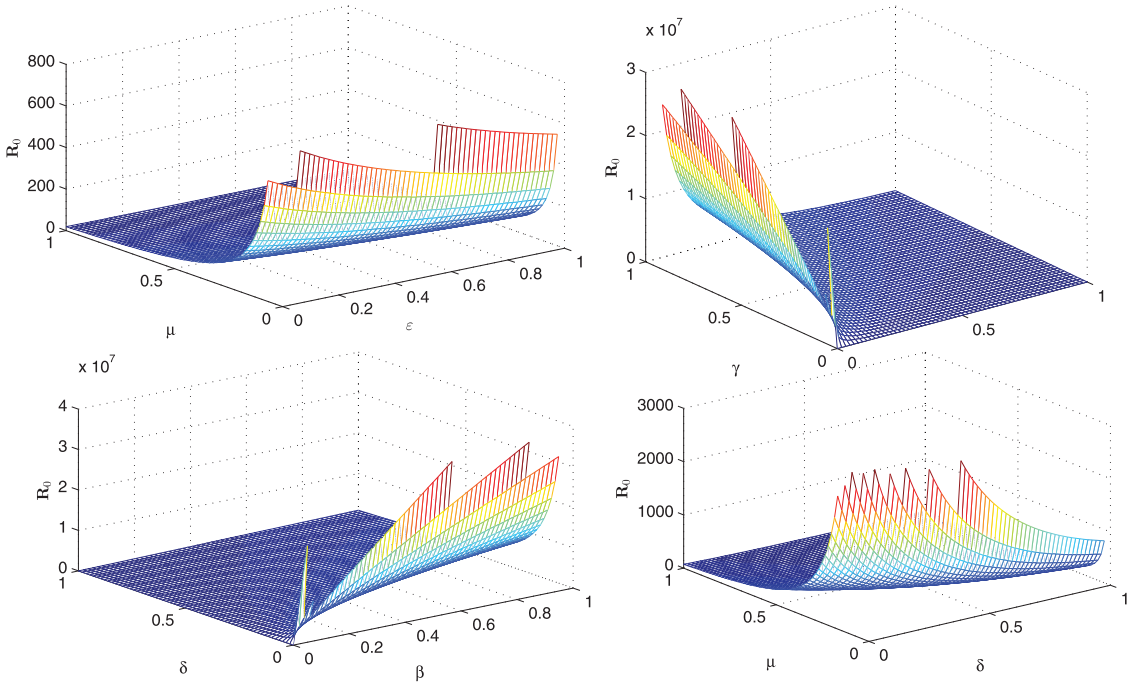

Figure 2: 3D configuration of $\mathbf{R}_0$ against different parameters of the model with $\mathbf{N} = 100$ millions

Lemma 4.1. Inview of Lemma 3.1, the solution of

$$
\begin{aligned}
&{}_{0}^{PC}D_{t}^{\alpha}\mathbf{g}(t) = \mathbf{F}\left(t, \mathbf{g}\left(t\right)\right), 0 < \alpha \leq 1,\ t \in [0, t_2] \\
&\mathbf{g}(0) = \mathbf{g}_0
\end{aligned}
$$

is given by

$$
\mathbf{g}\left(t\right) = \begin{cases} \mathbf{g}_0 + \int_0^t \mathbf{F}(\tau, \mathbf{g}(\tau))d\tau, 0 < t \leq t_1, \\ \mathbf{g}\left(t_1\right) + \dfrac{1}{\Gamma(\alpha)} \int_{t_1}^{t_2} (t-\tau)^{\alpha-1} \mathbf{F}\left(\tau, \mathbf{g}\left(\tau\right)\right) d\left(\tau\right),\ t_1 < t \leq t_2, \end{cases} \tag{4}
$$

where

$$
\mathbf{g}(t) = \begin{cases} \mathbf{S}(t) \\ \mathbf{E}(t) \\ \mathbf{I}(t) \\ \mathbf{T}(t) \\ \mathbf{R}(t) \end{cases}, \quad \mathbf{g}_0 = \begin{cases} \mathbf{S}_0 \\ \mathbf{E}_0 \\ \mathbf{I}_0 \\ \mathbf{T}_0 \\ \mathbf{R}_0 \end{cases}, \quad \mathbf{g}(t_1) = \begin{cases} \mathbf{S}(t_1) \\ \mathbf{E}(t_1) \\ \mathbf{I}(t_1) \\ \mathbf{T}(t_1) \\ \mathbf{R}(t_1) \end{cases}, \quad \mathbf{F}(t, \mathbf{g}(t)) = \begin{cases} \mathbf{F}_1(t, \mathbf{g}(t)) = \begin{cases} \mathbf{F}_1(\mathbf{S}, \mathbf{E}, \mathbf{I}, \mathbf{T}, \mathbf{R}, t), 0 < t < t_1, \\ \mathbf{F}_1(\mathbf{S}, \mathbf{E}, \mathbf{I}, \mathbf{T}, \mathbf{R}, t), t_1 < t \leq t_2, \end{cases} \\ \mathbf{F}_2(t, \mathbf{g}(t)) = \begin{cases} \mathbf{F}_2(\mathbf{S}, \mathbf{E}, \mathbf{I}, \mathbf{T}, \mathbf{R}, t), 0 < t < t_1, \\ \mathbf{F}_2(\mathbf{S}, \mathbf{E}, \mathbf{I}, \mathbf{T}, \mathbf{R}, t), t_1 < t \leq t_2, \end{cases} \\ \mathbf{F}_3(t, \mathbf{g}(t)) = \begin{cases} \mathbf{F}_3(\mathbf{S}, \mathbf{E}, \mathbf{I}, \mathbf{T}, \mathbf{R}, t), 0 < t < t_1, \\ \mathbf{F}_3(\mathbf{S}, \mathbf{E}, \mathbf{I}, \mathbf{T}, \mathbf{R}, t), t_1 < t \leq t_2, \end{cases} \\ \mathbf{F}_4(t, \mathbf{g}(t)) = \begin{cases} \mathbf{F}_4(\mathbf{S}, \mathbf{E}, \mathbf{I}, \mathbf{T}, \mathbf{R}, t), 0 < t < t_1, \\ \mathbf{F}_4(\mathbf{S}, \mathbf{E}, \mathbf{I}, \mathbf{T}, \mathbf{R}, t), t_1 < t \leq t_2. \end{cases} \\ \mathbf{F}_5(t, \mathbf{g}(t)) = \begin{cases} \mathbf{F}_5(\mathbf{S}, \mathbf{E}, \mathbf{I}, \mathbf{T}, \mathbf{R}, t), 0 < t < t_1, \\ \mathbf{F}_5(\mathbf{S}, \mathbf{E}, \mathbf{I}, \mathbf{T}, \mathbf{R}, t), t_1 < t \leq t_2. \end{cases} \end{cases} \tag{5}
$$

Proof. Following the fashion of Lemma 3.1, we can easily obtain the solution above. Let $\mathscr{E}$ be the space of all piecewise differentiable functions from $[0, t_2]$ to R, then obviously it is a complete normed space and hence the Banach space is expressed by $\mathscr{E} = C[0, t_2]$, where $0 < t_2 < \infty$ with the norm

$$\|\mathbf{g}\| = \max_{t \in [0, t_2]} |\mathbf{g}(t)|.$$

We use the growth and Lipschtiz conditions on the non-linear operator **F** to achieve the desired objectives.

(D1) Let $L_{\mathbf{F}} > 0$ be the Lipschitz constant and $\mathbf{g}, \overline{\mathbf{g}} \in \mathscr{E}$, then the following holds

$$|\mathbf{F}\left(t, \mathbf{g}\right) - \mathbf{F}\left(t, \overline{\mathbf{g}}\right)| \leq L_{\mathbf{F}} |\mathbf{g} - \overline{\mathbf{g}}|.$$

(D2) If $C_{\mathbf{F}} > 0$ and $M_{\mathbf{F}} > 0$, then the following holds

$$|\mathbf{F}(t, \mathbf{g}(t))| \leq C_{\mathbf{F}} |\mathbf{g}| + M_{\mathbf{F}}.$$

Theorem 4.2. Let piece-wise continuous function **F** be on the sub-intervals $0 < t \leq t_1$ and $t_1 < t \leq t_2$ of the interval $[0, T]$ and also if the hypothesis $(D2)$ holds, then the system (2) will have at least one solution.

Proof. Using Schauder fixed point theorem, let denote a closed and bounded subset $\mathscr{B}$ of $\mathscr{E}$ as $\mathscr{B} = \{\mathbf{g} \in \mathscr{E} : \|\mathbf{g}\| \leq \mathscr{R}_{1,2}, \mathscr{R}_{1,2} > 0\}$.

Let $\mathscr{T}:\mathscr{B}\to\mathscr{B}$ using (4), then

$$\mathscr{T}(\mathbf{g})=\begin{cases}\mathbf{g}_0+\int_0^t \mathbf{F}(\tau,\mathbf{g}(\tau))d\tau, 0<\mathrm{t}\le \mathrm{t}_1,\\ \mathbf{g}(\mathrm{t}_1)+\dfrac{1}{\Gamma\alpha}\int_{\mathrm{t}_1}^{\mathrm{t}_2}(\mathrm{t}-\tau)^{\alpha-1}\mathbf{F}(\tau,\mathbf{g}(\tau))\,d(\tau),\ \mathrm{t}_1<\mathrm{t}\le \mathrm{t}_2.\end{cases} \tag{6}$$

For $\mathbf{g}\in\mathscr{B}$, it follows that

$$\begin{aligned}|\mathscr{T}(\mathbf{g})(t)|&\le\begin{cases}|\mathbf{g}_0|+\int_0^{\mathrm{t}_1}|\mathbf{F}(\tau,\mathbf{g}(\tau))|\mathrm{d}\tau,\\ |\mathbf{g}(\mathrm{t}_1)|+\dfrac{1}{\Gamma(\alpha)}\int_{\mathrm{t}_1}^{\mathrm{t}_2}(\mathrm{t}-\tau)^{\alpha-1}|\mathbf{F}(\tau,\mathbf{g}(\tau))|\mathrm{d}(\tau),\end{cases}\\ &\le\begin{cases}|\mathbf{g}_0|+\int_0^{\mathrm{t}_1}[\mathrm{C}_{\mathbf{F}}|\mu|+\mathrm{M}_{\mathbf{F}}]d\tau,\\ |\mathbf{g}(\mathrm{t}_1)|+\dfrac{1}{\Gamma(\alpha)}\int_{\mathrm{t}_1}^{\mathrm{t}_2}(\mathrm{t}-\tau)^{\alpha-1}[\mathrm{C}_{\mathbf{F}}|\mathbf{g}|+\mathrm{M}_{\mathbf{F}}]d(\tau),\end{cases}\\ &\le\begin{cases}|\mathbf{g}_0|+\mathrm{t}_1[\mathrm{C}_{\mathbf{F}}\mathscr{R}_{1,2}+\mathrm{M}_{\mathbf{F}}]\le\mathscr{R}_{1,2}, 0<\mathrm{t}\le\mathrm{t}_1,\\ |\mathbf{g}(\mathrm{t}_1)|+\dfrac{\mathrm{t}_2^{\alpha}}{\Gamma(\alpha+1)}[\mathscr{C}_{\mathbf{F}}\mathscr{R}_{1,2}+\mathscr{M}_F]\le\mathscr{R}_{1,2},\ \mathrm{t}_1<\mathrm{t}\le\mathrm{t}_2,\end{cases}\end{aligned}$$

for $\mathrm{t}_1<\mathrm{t}<\le\mathrm{t}_2$, using $|(\mathrm{t}_1-\tau)^{\alpha}-(\mathrm{t}_2-\tau)^{\alpha}|\le\mathrm{t}_2^{\alpha}$, one has

$$\mathscr{R}_{1,2}\ge\max\begin{cases}\dfrac{|\mathbf{g}_0|+\mathrm{t}_1\mathrm{M}_{\mathbf{F}}}{1-\mathrm{t}_1\mathrm{C}_F}, & 0<\mathrm{t}\le\mathrm{t}_1,\\ \dfrac{|\mathbf{g}(\mathrm{t}_1)|\Gamma(\alpha+1)+\mathrm{t}_2^{\alpha}\mathscr{M}_{\mathbf{F}}}{(\Gamma(\alpha+1)-\mathrm{t}_2^{\alpha}\mathrm{C}_{\mathbf{F}}}, & \mathrm{t}_1<\mathrm{t}\le\mathrm{t}_2.\end{cases}$$

Thus, it proved that $\|\mathscr{T}(\mathbf{g})\|\le\mathscr{R}_{1,2}$, which further implies that $\mathscr{T}$ is bounded. Also, $\mathscr{T}(\mathscr{B})\subset\mathscr{B}$. Hence, $\mathscr{T}$ maps bounded set. For continuity, we use $\mathrm{t}_{\mathrm{m}}<\mathrm{t}_{\mathrm{n}}\in[0,\mathrm{t}_1]$ and take a classical derivative case first

$$\begin{aligned}|\mathscr{T}(\mathbf{g})(\mathrm{t}_{\mathrm{n}})-\mathscr{T}(\mathbf{g})(\mathrm{t}_{\mathrm{m}})|&=\left|\int_0^{\mathrm{t}_{\mathrm{n}}}\mathbf{F}(\tau,\mathbf{g}(\tau))\,d\tau-\int_0^{\mathrm{t}_{\mathrm{m}}}\mathbf{F}(\tau,\mathbf{g}(\tau))\,d\tau\right|\\ &\le\int_{\mathrm{t}_{\mathrm{m}}}^{\mathrm{t}_{\mathrm{n}}}|\mathbf{F}(\tau,\mathbf{g}(\tau))|d\tau\\ &\le\int_{\mathrm{t}_{\mathrm{m}}}^{\mathrm{t}_{\mathrm{n}}}[\mathrm{C}_{\mathbf{F}}|\mathbf{g}|+\mathscr{M}_{\mathbf{F}}]d\tau\\ &\le(\mathrm{C}_{\mathbf{F}}\mathscr{R}_{1,2},+\mathscr{M}_{\mathbf{F}})[\mathrm{t}_{\mathrm{n}}-\mathrm{t}_{\mathrm{m}}].\end{aligned} \tag{7}$$

By (7), we obtain $\mathrm{t}_{\mathrm{m}}\to\mathrm{t}_{\mathrm{n}}$ which yields

$$|\mathscr{T}(\mathbf{g})(\mathrm{t}_{\mathrm{n}})-\mathscr{T}(\mathbf{g})(\mathrm{t}_{\mathrm{m}})|\to 0,\ \text{as}\ \mathrm{t}_{\mathrm{m}}\to\mathrm{t}_{\mathrm{n}}.$$

Since $\mathscr{T}$ is uniformly continuous and bounded on the interval $[0,\mathrm{t}_1]$ interval, it implies

$$\|\mathscr{T}(\mathbf{g})(\mathrm{t}_{\mathrm{n}})-\mathscr{T}(\mathbf{g})(\mathrm{t}_{\mathrm{m}})\|\to 0,\ \text{as}\ \mathrm{t}_{\mathrm{m}}\to\mathrm{t}_{\mathrm{n}}.$$

It follows that $\mathscr{T}$ is equi-continuous in this case.

Next, we take the other interval $t_m < t_n \in (t_1, t_2]$ as

$$
\begin{aligned}
|\mathscr{T}(\mathbf{g})(t_n) - \mathscr{T}(\mathbf{g})(t_m)| &= \left| \frac{1}{\Gamma(\alpha)} \int_0^{t_n} (t_n - \tau)^{\alpha-1} F(\tau, g(\tau))\, d\tau - \frac{1}{\Gamma(\alpha)} \int_0^{t_m} (t_m - \tau)^{\alpha-1} F(\tau, \mathbf{g}(\tau))\, d\tau \right| \\
&\leq \frac{1}{\Gamma(\alpha)} \int_0^{t_m} \left[(t_m - \tau)^{\alpha-1} - (t_n - \tau)^{\alpha-1} \right] |\mathbf{F}(\tau, \mathbf{g}(\tau))|\, d\tau \\
&+ \frac{1}{\Gamma(\alpha)} \int_{t_m}^{t_n} (t_n - \tau)^{\alpha-1} |\mathbf{F}(\tau, \mathbf{g}(\tau))|\, d\tau \\
&\leq \frac{1}{\Gamma(\alpha)} \left[\int_0^{t_m} \left[(t_m - \tau)^{\alpha-1} - (t_n - \tau)^{\alpha-1} \right] d\tau \right. \\
&+ \left. \int_{t_m}^{t_n} (t_n - \tau)^{\alpha-1} d\tau \right] (C_{\mathbf{F}} |\mathbf{g}| + \mathscr{M}_{\mathbf{F}}) \\
&\leq \frac{(C_{\mathbf{F}} \mathscr{R}_{1,2} + \mathscr{M}_{\mathbf{F}})}{\Gamma(\alpha + 1)} \left[t_n^{\alpha} - t_m^{\alpha} + 2 (t_n - t_m)^{\alpha} \right]. \qquad (8)
\end{aligned}
$$

We see from (8), that

$$|\mathscr{T}(\mathbf{g})(t_n) - \mathscr{T}(\mathbf{g})(t_m)| \to 0, \text{ as } t_m \to t_n.$$

$\mathscr{T}$ is bounded on the interval $(t_1, t_2]$ and also uniformly continuous. Thus,

$$\|\mathscr{T}(\mathbf{g})(t_n) - \mathscr{T}(\mathbf{g})(t_m)\| \to 0, \text{ as } t_m \to t_n.$$

Hence, $\mathscr{T}$ is equi-continuous on the interval $(t_1, t_2]$.

Therefore, $\mathscr{T}$ is equi-continuous mapping over $[0, t_1] \cup (t_1, t_2]$. On using the Arzelá-Ascoli theorem [39], which states if the operator is relatively compact, then it will be completely continuous. Hence, $\mathscr{T}$ is completely continuous. Moreover, by using Schauder's fixed point theorem [40], the suggested model (2) has at least one solution.

Theorem 4.3. By hypothesis $(D1)$, if $t_2^{\alpha} < \frac{\Gamma(\alpha+1)}{L_{\mathbf{F}}}$, then the proposed model under piecewise derivative has a unique approximate solution.

Proof. Consider the mapping $\mathscr{T} : \mathscr{E} \to \mathscr{E}$, and if $\mathbf{g}, \bar{\mathbf{g}} \in \mathscr{E}$, then in case of $[0, t_1]$, one has

$$
\begin{aligned}
\|\mathscr{T}(\mathbf{g}) - \mathscr{T}(\bar{\mathbf{g}})\| &= \max_{t \in [0,t_1]} \left| \int_0^{t_1} \mathbf{F}(\tau, \mathbf{g}(\tau))\, d\tau - \int_0^{t_1} \mathbf{F}(\tau, \bar{\mathbf{g}}(\tau))\, d\tau \right| \\
&\leq t_1 L_{\mathbf{F}} \|\mathbf{g} - \bar{\mathbf{g}}\|. \qquad (9)
\end{aligned}
$$

Using (9), one has

$$\|\mathscr{T}(\mathbf{g}) - \mathscr{T}(\bar{\mathbf{g}})\| \leq t_1 L_{\mathbf{F}} \|\mathbf{g} - \bar{\mathbf{g}}\|. \qquad (10)$$

For $t \in (t_1, t_2]$ in the Caputo sense of derivative, we get from (10)

$$
\begin{aligned}
\|\mathscr{T}(\mathbf{g}) - \mathscr{T}(\bar{\mathbf{g}})\| &= \max_{t \in (t_1,t_2]} \left| \frac{1}{\Gamma(\alpha)} \int_{t_1}^{t_2} (t - \tau)^{\alpha-1} \mathbf{F}(\tau, \mathbf{g}(\tau))\, d\tau - \frac{1}{\Gamma(\alpha)} \int_{t_1}^{t_2} (t - \tau)^{\alpha-1} \mathbf{F}(\tau, \bar{\mathbf{g}}(\tau))\, d\tau \right| \\
&\leq \frac{t_2^{\alpha}}{\Gamma(\alpha + 1)} L_{\mathbf{F}} \|\mathbf{g} - \bar{\mathbf{g}}\|. \qquad (11)
\end{aligned}
$$

From Eq. (11), we get

$$\| \mathscr{T}(\mathbf{g}) - \mathscr{T}(\bar{\mathbf{g}}) \| \leq \frac{t_2^{\alpha}}{\Gamma(\alpha+1)} L_{\mathbf{F}} \| \mathbf{g} - \bar{\mathbf{g}} \|.$$

Therefore, $\mathscr{T}$ is a contraction operator in both cases. As a conclusion, the suggested model has a unique approximate solution under piecewise derivative.

5 Numerical Scheme

For piecewise derivable problem (2), we develop a numerical technique for the two sub-intervals of $[0, t_2]$ in order to perform numerical results. For the piecewise problem, the numerical algorithm will be the same as the integer order numerical algorithm defined in [24]. We remark that the Adams-Bashforth method preserves the basic type of numerical stability associated with the usual one-step numerical methods, including Euler, backward Euler, trapezoidal, etc. Further, it is a $(l+1)$-step explicit method, whose truncation error is of size $O(h^{l+2})$. For detailed convergence and stability of the Adams-Bashforth method, we refer to the reference [42] for further detail.

The solution of (2) under the piecewise derivative can be expressed as

$$\mathbf{S}(t) = \begin{cases} \mathbf{S}_0 + \int_0^{t_1} \mathbf{F}_1(\mathbf{S},\mathbf{E},\mathbf{I},\mathbf{T},\mathbf{R},\tau)d\tau, 0 < t \leq t_1, \\ \mathbf{S}(t_1) + \frac{1}{\Gamma(\alpha)} \int_{t_1}^{t_2} (t-\tau)^{\alpha-1} \mathbf{F}_1(\mathbf{S},\mathbf{E},\mathbf{I},\mathbf{T},\mathbf{R},\tau)\, d\tau, \ t_1 < t \leq t_2, \end{cases},$$

$$\mathbf{E}(t) = \begin{cases} \mathbf{E}_0 + \int_0^{t_1} \mathbf{F}_2(\mathbf{S},\mathbf{E},\mathbf{I},\mathbf{T},\mathbf{R},\tau)d\tau, 0 < t \leq t_1, \\ \mathbf{E}(t_1) + \frac{1}{\Gamma(\alpha)} \int_{t_1}^{t_2} (t-\tau)^{\alpha-1} \mathbf{F}_2(\mathbf{S},\mathbf{E},\mathbf{I},\mathbf{T},\mathbf{R},\tau)\, d\tau, \ t_1 < t \leq t_2, \end{cases},$$

$$\mathbf{I}(t) = \begin{cases} \mathbf{I}_0 + \int_0^{t_1} \mathbf{F}_3(\mathbf{S},\mathbf{E},\mathbf{I},\mathbf{T},\mathbf{R},\tau)d\tau, 0 < t \leq t_1, \\ \mathbf{I}(t_1) + \frac{1}{\Gamma(\alpha)} \int_{t_1}^{t_2} (t-\tau)^{\alpha-1} \mathbf{F}_3(\mathbf{S},\mathbf{E},\mathbf{I},\mathbf{T},\mathbf{R},\tau)\, d\tau, \ t_1 < t \leq t_2, \end{cases},$$

$$\mathbf{T}(t) = \begin{cases} \mathbf{T}_0 + \int_0^{t_1} \mathbf{F}_4(\mathbf{S},\mathbf{E},\mathbf{I},\mathbf{T},\mathbf{R},\tau)d\tau, 0 < t \leq t_1, \\ \mathbf{T}(t_1) + \frac{1}{\Gamma(\alpha)} \int_{t_1}^{t_2} (t-\tau)^{\alpha-1} \mathbf{F}_4(\mathbf{S},\mathbf{E},\mathbf{I},\mathbf{T},\mathbf{R},\tau)\, d\tau, \ t_1 < t \leq t_2, \end{cases},$$

$$\mathbf{R}(t) = \begin{cases} \mathbf{R}_0 + \int_0^{t_1} \mathbf{F}_5(\mathbf{S},\mathbf{E},\mathbf{I},\mathbf{T},\mathbf{R},\tau)d\tau, 0 < t \leq t_1, \\ \mathbf{R}(t_1) + \frac{1}{\Gamma(\alpha)} \int_{t_1}^{t_2} (t-\tau)^{\alpha-1} \mathbf{F}_5(\mathbf{S},\mathbf{E},\mathbf{I},\mathbf{T},\mathbf{R},\tau)\, d\tau, \ t_1 < t \leq t_2. \end{cases} \tag{12}$$

We will first develop the strategy for the first equation in System (12) and then apply it to the rest of the equations. At $t = t_{n+1}$, then we have

$$\mathbf{S}(t_{n+1}) = \begin{cases} \mathbf{S}_0 + \int_0^{t_1} \mathbf{F}_1(\mathbf{S},\mathbf{E},\mathbf{I},\mathbf{T},\mathbf{R},\tau)d\tau, & 0 < t \leq t_1, \\ \mathbf{S}(t_1) + \frac{1}{\Gamma(\alpha)} \int_{t_1}^{t_{n+1}} (t-\tau)^{\alpha-1} \mathbf{F}_1(\mathbf{S},\mathbf{E},\mathbf{I},\mathbf{T},\mathbf{R},\tau)\, d\tau, & t_1 < t \leq t_2, \end{cases} \tag{13}$$

Eq. (13) is expressed in the Newton interpolation formula given in the reference as

$$
\begin{aligned}
&\mathbf{S}(t_{n+1}) \\
&= \left\{ \begin{array}{l}
\mathbf{S}_0 + \left\{ \begin{array}{l}
\sum_{k=2}^{i} \left[\frac{5}{12}\mathbf{F}_1(\mathbf{S}^{k-2}, \mathbf{E}^{k-2}, \mathbf{I}^{k-2}, \mathbf{T}^{k-2}, \mathbf{R}^{k-2}, t_{k-2})\Delta t \right. \\
\left. -\frac{4}{3}\mathbf{F}_1(\mathbf{S}^{k-1}, \mathbf{E}^{k-1}, \mathbf{I}^{k-1}, \mathbf{T}^{k-1}, \mathbf{R}^{k-1}, t_{k-1})\Delta t + \mathbf{F}_1(\mathbf{S}^{k}, \mathbf{E}^{k}, \mathbf{I}^{k}, \mathbf{T}^{k}, \mathbf{R}^{k}, t_{k}) \right],
\end{array} \right. \\
\mathbf{S}(t_1) + \left\{ \begin{array}{l}
\frac{(\Delta t)^{\alpha-1}}{\Gamma(\alpha+1)} \sum_{k=i+3}^{n} [\mathbf{F}_1(\mathbf{S}^{k-2}, \mathbf{E}^{k-2}, \mathbf{I}^{k-2}, \mathbf{T}^{k-2}, \mathbf{R}^{k-2}, t_{k-2})][(n-k+1)^{\alpha}(n-k)^{\alpha}] \\
+\frac{(\Delta t)^{\alpha-1}}{\Gamma(\alpha+2)} \sum_{k=i+3}^{n} [\mathbf{F}_1(\mathbf{S}^{k-1}, \mathbf{E}^{k-1}, \mathbf{I}^{k-1}, \mathbf{T}^{k-1}, \mathbf{R}^{k-1}, t_{k-1}) \\
-\mathbf{F}_1(\mathbf{S}^{k-2}, \mathbf{E}^{k-2}, \mathbf{I}^{k-2}, \mathbf{T}^{k-2}, \mathbf{R}^{k-2}, t_{k-2})] \times \\
[(n-k+1)^{\alpha}(n-k+3+2\alpha) - (n-k)(n-k+3+3\alpha)] \\
+\frac{\alpha(\Delta t)^{\alpha-1}}{2\Gamma(\alpha+3)} \sum_{k=i+3}^{n} [\mathbf{F}_1(\mathbf{S}^{k}, \mathbf{E}^{k}, \mathbf{I}^{k}, \mathbf{T}^{k}, \mathbf{R}^{k}, t_{k}) - 2\mathbf{F}_1(\mathbf{S}^{k-1}, \mathbf{E}^{k-1}, \mathbf{I}^{k-1}, \mathbf{T}^{k-1}, \mathbf{R}^{k-1}, t_{k-1}) \\
+\mathbf{F}_1(\mathbf{S}^{k-2}, \mathbf{E}^{k-2}, \mathbf{I}^{k-2}, \mathbf{T}^{k-2}, \mathbf{R}^{k-2}, t_{k-2})] \\
\times [(n-k+1)^{\alpha}(2(n-k)^2 + (3\alpha+10)(n-k) + 2\alpha^2 + 9\alpha + 12) - (n-k)^{\alpha}(2(n-k)^2) \\
+((5\alpha+10)(n-k) + 6\alpha^2 + 18\alpha + 12))]
\end{array} \right.
\end{array} \right.
\end{aligned}
\tag{14}
$$

For the rest of three equations, we can write the Newton interpolation scheme as shown below:

$$
\begin{aligned}
&\mathbf{E}(t_{n+1}) \\
&= \left\{ \begin{array}{l}
\mathbf{E}_0 + \left\{ \begin{array}{l}
\sum_{k=2}^{i} \left[\frac{5}{12}\mathbf{F}_2(\mathbf{S}^{k-2}, \mathbf{E}^{k-2}, \mathbf{I}^{k-2}, \mathbf{T}^{k-2}, \mathbf{R}^{k-2}, t_{k-2})\Delta t \right. \\
\left. -\frac{4}{3}\mathbf{F}_2(\mathbf{S}^{k-1}, \mathbf{E}^{k-1}, \mathbf{I}^{k-1}, \mathbf{T}^{k-1}, \mathbf{R}^{k-1}, t_{k-1})\Delta t + \mathbf{F}_2(\mathbf{S}^{k}, \mathbf{E}^{k}, \mathbf{I}^{k}, \mathbf{T}^{k}, \mathbf{R}^{k}, t_{k}) \right],
\end{array} \right. \\
\mathbf{E}(t_1) + \left\{ \begin{array}{l}
\frac{(\Delta t)^{\alpha-1}}{\Gamma(\alpha+1)} \sum_{k=i+3}^{n} [\mathbf{F}_2(\mathbf{S}^{k-2}, \mathbf{E}^{k-2}, \mathbf{I}^{k-2}, \mathbf{T}^{k-2}, \mathbf{R}^{k-2}, t_{k-2})][(n-k+1)^{\alpha}(n-k)^{\alpha}] \\
+\frac{(\Delta t)^{\alpha-1}}{\Gamma(\alpha+2)} \sum_{k=i+3}^{n} [\mathbf{F}_2(\mathbf{S}^{k-1}, \mathbf{E}^{k-1}, \mathbf{I}^{k-1}, \mathbf{T}^{k-1}, \mathbf{R}^{k-1}, t_{k-1}) \\
-\mathbf{F}_2(\mathbf{S}^{k-2}, \mathbf{E}^{k-2}, \mathbf{I}^{k-2}, \mathbf{T}^{k-2}, \mathbf{R}^{k-2}, t_{k-2})] \times \\
[(n-k+1)^{\alpha}(n-k+3+2\alpha) - (n-k)(n-k+3+3\alpha)] \\
+\frac{\alpha(\Delta t)^{\alpha-1}}{2\Gamma(\alpha+3)} \sum_{k=i+3}^{n} [\mathbf{F}_2(\mathbf{S}^{k}, \mathbf{E}^{k}, \mathbf{I}^{k}, \mathbf{T}^{k}, \mathbf{R}^{k}, t_{k}) - 2\mathbf{F}_2(\mathbf{S}^{k-1}, \mathbf{E}^{k-1}, \mathbf{I}^{k-1}, \mathbf{T}^{k-1}, \mathbf{R}^{k-1}, t_{k-1}) \\
+\mathbf{F}_2(\mathbf{S}^{k-2}, \mathbf{E}^{k-2}, \mathbf{I}^{k-2}, \mathbf{T}^{k-2}, \mathbf{R}^{k-2}, t_{k-2})] \\
\times [(n-k+1)^{\alpha}(2(n-k)^2 + (3\alpha+10)(n-k) + 2\alpha^2 + 9\alpha + 12) - (n-k)^{\alpha}(2(n-k)^2) \\
+((5\alpha+10)(n-k) + 6\alpha^2 + 18\alpha + 12))]
\end{array} \right.
\end{array} \right.
\end{aligned}
\tag{15}
$$

$$\mathbf{I}(\mathrm{t}_{n+1})$$

$$= \begin{Bmatrix} \mathbf{I}_0 + \begin{Bmatrix} \sum_{\mathrm{k}=2}^{\mathrm{i}} \Big[\frac{5}{12}\mathbf{F}_3(\mathbf{S}^{\mathrm{k}-2}, \mathbf{E}^{\mathrm{k}-2}, \mathbf{I}^{\mathrm{k}-2}, \mathbf{T}^{\mathrm{k}-2}, \mathbf{R}^{\mathrm{k}-2}, \mathrm{t}_{\mathrm{k}-2})\Delta t \\ -\frac{4}{3}\mathbf{F}_3(\mathbf{S}^{\mathrm{k}-1}, \mathbf{E}^{\mathrm{k}-1}, \mathbf{I}^{\mathrm{k}-1}, \mathbf{T}^{\mathrm{k}-1}, \mathbf{R}^{\mathrm{k}-1}, \mathrm{t}_{\mathrm{k}-1})\Delta t + \mathbf{F}_3(\mathbf{S}^{\mathrm{k}}, \mathbf{E}^{\mathrm{k}}, \mathbf{I}^{\mathrm{k}}, \mathbf{T}^{k}, \mathbf{R}^{\mathrm{k}}, \mathrm{t}_{\mathrm{k}}) \Big], \\ \mathbf{I}(\mathrm{t}_1) + \begin{Bmatrix} \frac{(\Delta \mathrm{t})^{\alpha-1}}{\Gamma(\alpha+1)} \sum_{\mathrm{k}=\mathrm{i}+3}^{n} [\mathbf{F}_3(\mathbf{S}^{\mathrm{k}-2}, \mathbf{E}^{\mathrm{k}-2}, \mathbf{I}^{\mathrm{k}-2}, \mathbf{T}^{\mathrm{k}-2}, \mathbf{R}^{\mathrm{k}-2}, \mathrm{t}_{\mathrm{k}-2})][(n-\mathrm{k}+1)^{\alpha}(n-\mathrm{k})^{\alpha}] \\ +\frac{(\Delta t)^{\alpha-1}}{\Gamma(\alpha+2)} \sum_{\mathrm{k}=i+3}^{n} [\mathbf{F}_3(\mathbf{S}^{\mathrm{k}-1}, \mathbf{E}^{\mathrm{k}-1}, \mathbf{I}^{\mathrm{k}-1}, \mathbf{T}^{\mathrm{k}-1}, \mathbf{R}^{\mathrm{k}-1}, \mathrm{t}_{\mathrm{k}-1}) \\ -\mathbf{F}_3(\mathbf{S}^{\mathrm{k}-2}, \mathbf{E}^{\mathrm{k}-2}, \mathbf{I}^{\mathrm{k}-2}, \mathbf{T}^{\mathrm{k}-2}, \mathbf{R}^{\mathrm{k}-2}, \mathrm{t}_{\mathrm{k}-2})] \times \\ [(n-\mathrm{k}+1)^{\alpha}(n-\mathrm{k}+3+2\alpha) - (n-\mathrm{k})(n-\mathrm{k}+3+3\alpha)] \\ +\frac{\alpha(\Delta \mathrm{t})^{\alpha-1}}{2\Gamma(\alpha+3)} \sum_{\mathrm{k}=\mathrm{i}+3}^{n} [\mathbf{F}_3(\mathbf{S}^{\mathrm{k}}, \mathbf{E}^{\mathrm{k}}, \mathbf{I}^{\mathrm{k}}, \mathbf{T}^{\mathrm{k}}, \mathbf{R}^{\mathrm{k}}, t_{\mathrm{k}}) - 2\mathbf{F}_3(\mathbf{S}^{\mathrm{k}-1}, \mathbf{E}^{\mathrm{k}-1}, \mathbf{I}^{\mathrm{k}-1}, \mathbf{T}^{\mathrm{k}-1}, \mathbf{R}^{\mathrm{k}-1}, \mathrm{k}_{\mathrm{k}-1}) \\ +\mathbf{F}_3(\mathbf{S}^{\mathrm{k}-2}, \mathbf{E}^{\mathrm{k}-2}, \mathbf{I}^{\mathrm{k}-2}, \mathbf{T}^{\mathrm{k}-2}, \mathbf{R}^{\mathrm{k}-2}, \mathrm{t}_{\mathrm{k}-2})] \\ \times [(n-\mathrm{k}+1)^{\alpha}(2(n-\mathrm{k})^2 + (3\alpha+10)(n-\mathrm{k}) + 2\alpha^2 + 9\alpha + 12) - (n-\mathrm{k})^{\alpha}(2(n-\mathrm{k})^2) \\ +((5\alpha+10)(n-\mathrm{k}) + 6\alpha^2 + 18\alpha + 12))], \end{Bmatrix} \end{Bmatrix} \tag{16}$$

$$\mathbf{T}(t_{n+1})$$

$$= \begin{Bmatrix} \mathrm{t}_0 + \begin{Bmatrix} \sum_{\mathrm{k}=2}^{\mathrm{i}} \Big[\frac{5}{12}\mathbf{F}_4(\mathbf{S}^{\mathrm{k}-2}, \mathbf{E}^{\mathrm{k}-2}, \mathbf{I}^{\mathrm{k}-2}, \mathbf{T}^{\mathrm{k}-2}, \mathbf{R}^{\mathrm{k}-2}, \mathrm{t}_{\mathrm{k}-2})\Delta t \\ -\frac{4}{3}\mathbf{F}_4(\mathbf{S}^{\mathrm{k}-1}, \mathbf{E}^{\mathrm{k}-1}, \mathbf{I}^{\mathrm{k}-1}, \mathbf{T}^{\mathrm{k}-1}, \mathbf{R}^{\mathrm{k}-1}, \mathrm{t}_{\mathrm{k}-1})\Delta t + \mathbf{F}_4(\mathbf{S}^{\mathrm{k}}, \mathbf{E}^{\mathrm{k}}, \mathbf{I}^{\mathrm{k}}, \mathbf{T}^{\mathrm{k}}, \mathbf{R}^{\mathrm{k}}, t_{\mathrm{k}}) \Big], \\ \mathrm{t}(\mathrm{t}_1) + \begin{Bmatrix} \frac{(\Delta \mathrm{t})^{\alpha-1}}{\Gamma(\alpha+1)} \sum_{\mathrm{k}=\mathrm{i}+3}^{n} [\mathbf{F}_4(\mathbf{S}^{\mathrm{k}-2}, \mathbf{E}^{\mathrm{k}-2}, \mathbf{I}^{\mathrm{k}-2}, \mathbf{T}^{\mathrm{k}-2}, \mathbf{R}^{\mathrm{k}-2}, t_{\mathrm{k}-2})][(n-\mathrm{k}+1)^{\alpha}(n-\mathrm{k})^{\alpha}] \\ +\frac{(\Delta t)^{\alpha-1}}{\Gamma(\alpha+2)} \sum_{\mathrm{k}=i+3}^{n} [\mathbf{F}_4(\mathbf{S}^{\mathrm{k}-1}, \mathbf{E}^{\mathrm{k}-1}, \mathbf{I}^{\mathrm{k}-1}, \mathbf{T}^{\mathrm{k}-1}, \mathbf{R}^{\mathrm{k}-1}, \mathrm{k}_{\mathrm{k}-1}) \\ -\mathbf{F}_4(\mathbf{S}^{\mathrm{k}-2}, \mathbf{E}^{\mathrm{k}-2}, \mathbf{I}^{\mathrm{k}-2}, \mathbf{T}^{\mathrm{k}-2}, \mathbf{R}^{\mathrm{k}-2}, \mathrm{t}_{\mathrm{k}-2})] \times \\ [(n-\mathrm{k}+1)^{\alpha}(n-\mathrm{k}+3+2\alpha) - (n-\mathrm{k})(n-\mathrm{k}+3+3\alpha)] \\ +\frac{\alpha(\Delta t)^{\alpha-1}}{2\Gamma(\alpha+3)} \sum_{\mathrm{k}=\mathrm{i}+3}^{n} [\mathbf{F}_4(\mathbf{S}^{\mathrm{k}}, \mathbf{E}^{k}, \mathbf{I}^{\mathrm{k}}, \mathbf{T}^{\mathrm{k}}, \mathbf{R}^{\mathrm{k}}, t_{\mathrm{k}}) - 2\mathbf{F}_4(\mathbf{S}^{\mathrm{k}-1}, \mathbf{E}^{\mathrm{k}-1}, \mathbf{I}^{\mathrm{k}-1}, \mathbf{T}^{\mathrm{k}-1}, \mathbf{R}^{\mathrm{k}-1}, \mathrm{t}_{\mathrm{k}-1}) \\ +\mathbf{F}_4(\mathbf{S}^{\mathrm{k}-2}, \mathbf{E}^{\mathrm{k}-2}, \mathbf{I}^{\mathrm{k}-2}, \mathbf{T}^{\mathrm{k}-2}, \mathbf{R}^{\mathrm{k}-2}, \mathrm{t}_{\mathrm{k}-2})] \\ \times [(n-\mathrm{k}+1)^{\alpha}(2(n-\mathrm{k})^2 + (3\alpha+10)(n-\mathrm{k}) + 2\alpha^2 + 9\alpha + 12) - (n-\mathrm{k})^{\alpha}(2(n-\mathrm{k})^2) \\ +((5\alpha+10)(n-\mathrm{k}) + 6\alpha^2 + 18\alpha + 12))], \end{Bmatrix} \end{Bmatrix} \tag{17}$$

and

$$\mathbf{R}(\mathrm{t}_{n+1})$$

$$= \left\{ \begin{array}{l} \mathbf{R}_0 + \left\{ \begin{array}{l} \sum\limits_{\mathrm{k}=2}^{\mathrm{i}} \left[\frac{5}{12}\mathbf{F}_5(\mathbf{S}^{\mathrm{k}-2}, \mathbf{E}^{\mathrm{k}-2}, \mathbf{I}^{\mathrm{k}-2}, \mathbf{T}^{\mathrm{k}-2}, \mathbf{R}^{\mathrm{k}-2}, \mathrm{t}_{\mathrm{k}-2})\Delta t \right. \\ \left. -\frac{4}{3}\mathbf{F}_5(\mathbf{S}^{\mathrm{k}-1}, \mathbf{E}^{\mathrm{k}-1}, \mathbf{I}^{\mathrm{k}-1}, \mathbf{T}^{\mathrm{k}-1}, \mathbf{R}^{\mathrm{k}-1}, \mathrm{t}_{\mathrm{k}-1})\Delta t + \mathbf{F}_5(\mathbf{S}^{\mathrm{k}}, \mathbf{E}^{\mathrm{k}}, \mathbf{I}^{\mathrm{k}}, \mathbf{T}^{\mathrm{k}}, \mathbf{R}^{k}, t_{\mathrm{k}}) \right], \end{array} \right. \\ \mathbf{R}(\mathrm{t}_1) + \left\{ \begin{array}{l} \frac{(\Delta \mathrm{t})^{\alpha-1}}{\Gamma(\alpha+1)} \sum\limits_{k=i+3}^{n} [\mathbf{F}_5(\mathbf{S}^{\mathrm{k}-2}, \mathbf{E}^{\mathrm{k}-2}, \mathbf{I}^{\mathrm{k}-2}, \mathbf{T}^{\mathrm{k}-2}, \mathbf{R}^{\mathrm{k}-2}, t_{\mathrm{k}-2})][(n-\mathrm{k}+1)^{\alpha}(n-\mathrm{k})^{\alpha}] \\ +\frac{(\Delta t)^{\alpha-1}}{\Gamma(\alpha+2)} \sum\limits_{\mathrm{k}=\mathrm{i}+3}^{n} [\mathbf{F}_5(\mathbf{S}^{\mathrm{k}-1}, \mathbf{E}^{\mathrm{k}-1}, \mathbf{I}^{\mathrm{k}-1}, \mathbf{T}^{\mathrm{k}-1}, \mathbf{R}^{\mathrm{k}-1}, t_{\mathrm{k}-1}) \\ -\mathbf{F}_5(\mathbf{S}^{\mathrm{k}-2}, \mathbf{E}^{\mathrm{k}-2}, \mathbf{I}^{\mathrm{k}-2}, \mathbf{T}^{\mathrm{k}-2}, \mathbf{R}^{\mathrm{k}-2}, t_{\mathrm{k}-2})] \times \\ [(n-\mathrm{k}+1)^{\alpha}(n-\mathrm{k}+3+2\alpha) - (n-\mathrm{k})(n-\mathrm{k}+3+3\alpha)] \\ +\frac{\alpha(\Delta \mathrm{t})^{\alpha-1}}{2\Gamma(\alpha+3)} \sum\limits_{\mathrm{k}=i+3}^{n} [\mathbf{F}_5(\mathbf{S}^{\mathrm{k}}, \mathbf{E}^{\mathrm{k}}, \mathbf{I}^{\mathrm{k}}, \mathbf{T}^{\mathrm{k}}, \mathbf{R}^{\mathrm{k}}, t_{\mathrm{k}}) - 2\mathbf{F}_5(\mathbf{S}^{\mathrm{k}-1}, \mathbf{E}^{\mathrm{k}-1}, \mathbf{I}^{\mathrm{k}-1}, \mathbf{T}^{k-1}, \mathbf{R}^{\mathrm{k}-1}, \mathrm{t}_{\mathrm{k}-1}) \\ +\mathbf{F}_5(\mathbf{S}^{\mathrm{k}-2}, \mathbf{E}^{\mathrm{k}-2}, \mathbf{I}^{\mathrm{k}-2}, \mathbf{T}^{\mathrm{k}-2}, \mathbf{R}^{\mathrm{k}-2}, \mathrm{t}_{\mathrm{k}-2})] \\ \times [(n-\mathrm{k}+1)^{\alpha}(2(n-\mathrm{k})^2 + (3\alpha+10)(n-\mathrm{k}) + 2\alpha^2 + 9\alpha + 12) - (n-\mathrm{k})^{\alpha}(2(n-\mathrm{k})^2) \\ +((5\alpha+10)(n-\mathrm{k}) + 6\alpha^2 + 18\alpha + 12))]. \end{array} \right. \end{array} \right. \tag{18}$$

6 Numerical Simulations and Discussion

We illustrate the numerical simulation in Figures utilizing the acquire scheme of Newton Polynomial of classical and global piece-wise derivative notion. We divide the interval into two sub-intervals and analyze the first for integer order derivatives, whereas the second is tested for different fractional orders in the sense of Caputo, using the data in a table. Here, we simulate our model corresponding to the numerical data given in Table 2. Here, we present approximate solutions under piecewise fractional order differentiation of the proposed model using various fractional orders. The concerned graphs for approximate solutions when $0 < \alpha \leq 0.6$ are given in Figs. 3–7. Those graphs where fractional order is $0.6 < \alpha \leq 1$ are presented in Figs. 8–12, respectively. By simulating the results with clear crossover (multi-steps) behaviors in various compartments and by splitting the whole domain [0, 30] into sub-intervals as $0 < \mathrm{t} \leq 5$ and $5 < \mathrm{t} \leq 30$, we see during treatment the corresponding population of susceptible, exposed, infected, treated, and recovered in the corresponding point appear to start a multi-step behavior. The decay process in smaller orders is faster while growth or raise occurs rapidly in larger fractional orders. The nature of the model under our study indicated a clear date when the infection transmitted from some infected sources to the healthy ones and also there is a termination if the infected ones got rid of disease either by treatment or death. Hence, the date of the evolution can be well known, more precisely as there is no peculiarity in the dynamic of the transmission, but a crossover behavior can be clearly observed in this case. The process is non-Markovian and has a crossover (multi-step) behavior. These remarks can be clearly understood from the Figs. 3–12. Initially, the population dynamics of each compartment are progressing normally, but after some sudden or abrupt changes occur, the dynamics of various compartments start multi-step behavior. Here, it should be kept in mind that such scenarios cannot be achieved by using usual fractional order or integer order derivatives.

Table 2: Numerical values with description and sources

Symbols	Descriptions	Numerical values	Source
S	Density of susceptible class	$\mathbf{S}_0 = 10$	[33]
E	Density of exposed class	$\mathbf{E}_0 = 1.5$	[33]
I	Density of infected class	$\mathbf{I}_0 = 1.3$	[33]
T	Density of treated class	$\mathbf{T}_0 = 1$	[33]
R	Density of recovered class	$\mathbf{R}_0 = 0.9$	[33]
Π	Birth rate	6100	[35]
β	Transmission rate	0.75	[36]
μ	Rate of natural death	0.000038642	[35]
ρ	Rate of death due to infection	0.76	[36]
Φ	The rate of the exposed population that becomes infected	0.60	[36]
ε_1	Rate of natural recovery in infected class	0.0054	[36]
ε_2	Rate of natural recovery in treatment class	0.0061	[36]
a	Rate of recovery	0.09	[36]
η	Infection rate	0.89	[35]
γ	The rate of progress from **I** to **T**	0.971	[36]
θ	Death rate of **T** due to infection	0.51	[35]
N	Number of total population	164,700,000	[33]

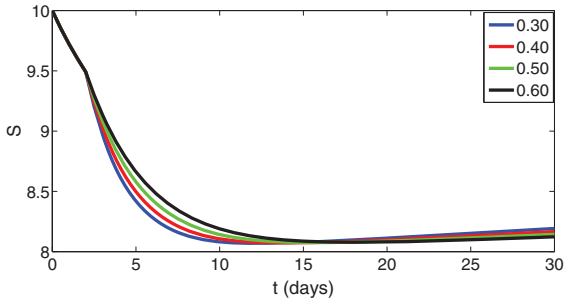

Figure 3: Graphical presentation of approximate solutions of susceptible compartment against different values of fractional orders such that $0 < \alpha \leq 0.6$

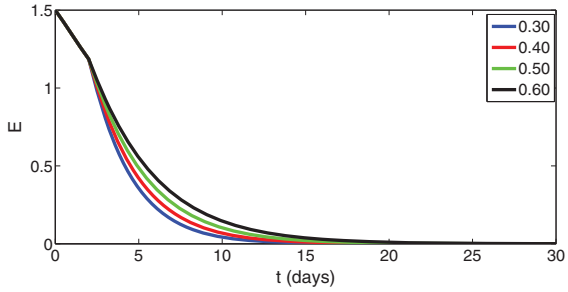

Figure 4: Graphical presentation of approximate solutions of exposed compartment against different values of fractional orders such that $0 < \alpha \leq 0.6$

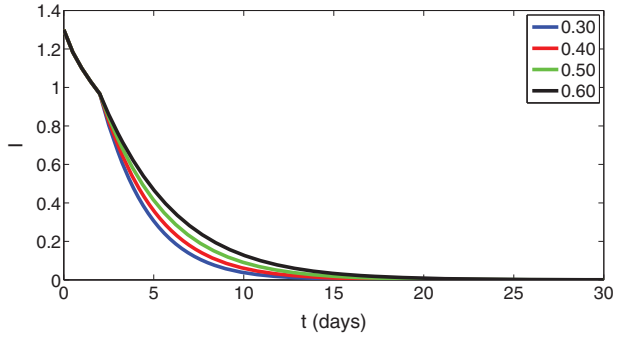

Figure 5: Graphical presentation of approximate solutions of infected compartment against different values of fractional orders such that $0 < \alpha \leq 0.6$

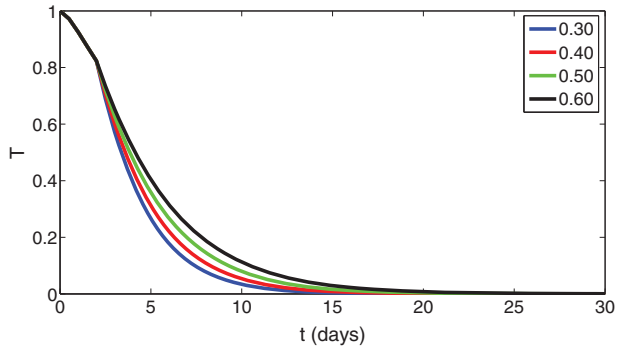

Figure 6: Graphical presentation of approximate solutions of treated compartment against different values of fractional orders such that $0 < \alpha \leq 0.6$

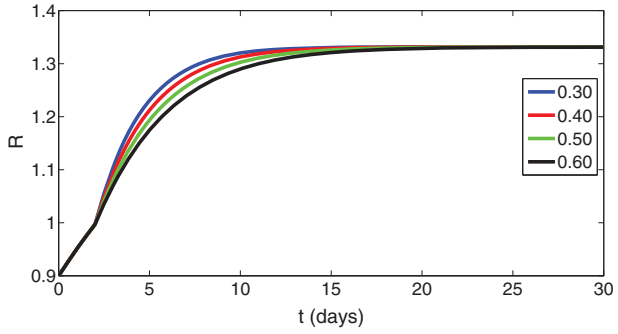

Figure 7: Graphical presentation of approximate solutions of recovered compartment against different values of fractional orders such that $0 < \alpha \leq 0.6$

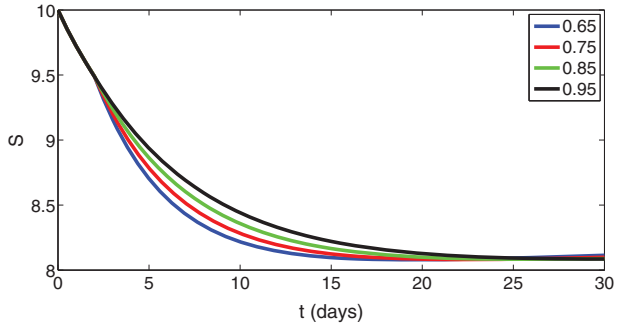

Figure 8: Graphical presentation of approximate solutions of susceptible compartment against different values of fractional orders such that $0.6 < \alpha \leq 1$

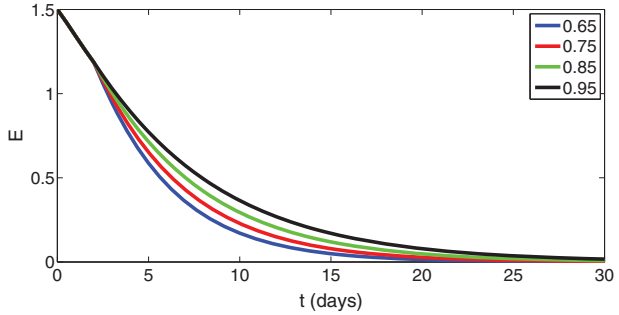

Figure 9: Graphical presentation of approximate solutions of exposed compartment against different values of fractional orders such that $0.6 < \alpha \leq 1$

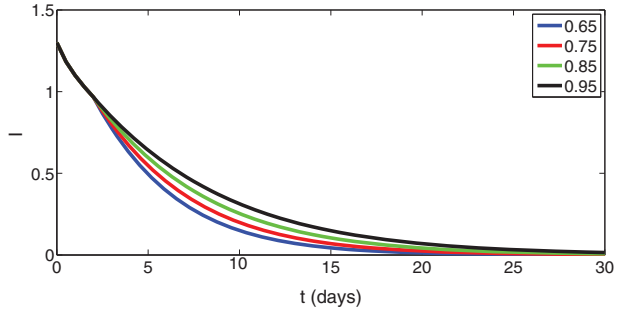

Figure 10: Graphical presentation of approximate solutions of infected compartment against different values of fractional orders such that $0.6 < \alpha \leq 1$

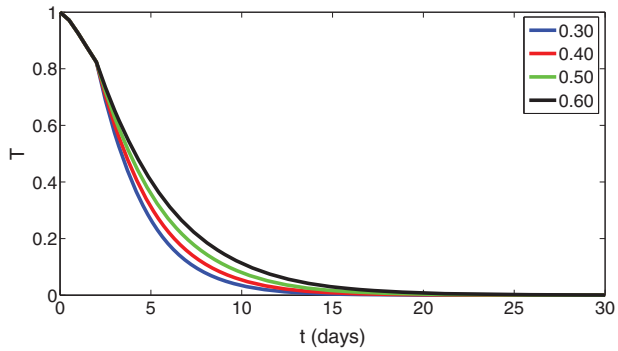

Figure 11: Graphical presentation of approximate solutions of treated compartment against different values of fractional orders such that $0.6 < \alpha \leq 1$

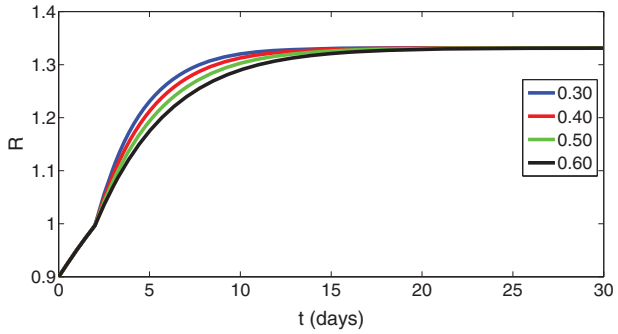

Figure 12: Graphical presentation of approximate solutions of recovered compartment against different values of fractional orders such that $0.6 < \alpha \leq 1$

7 Conclusion

In this article, we have developed a qualitative and computational analysis of a NiV disease. Based on the notion of the newly explored piecewise derivative of fractional order, we have investigated the model to study the crossover behavior in the dynamics of the disease. First of all, the invariance of the model and the feasible region has been established in the sense of the Caputo fractional derivative via using Laplace transform. Some remarks about thresholds number and their 3D profile corresponding to different parameters have been given. We have developed necessary and sufficient conditions for the existence and uniqueness of approximate solutions via fixed point results of Banach and Schauder. Utilizing the Newtonian polynomials of numerical interpolation, we have established algorithms for simulation purposes of the model. We have constructed the required scheme for numerical findings and their graphical presentation. We have simulated the model on different sets of fractional order by dividing the domain of time into two sub-intervals. Graphical presentations have indicated the crossover (multi-step) behavior in the dynamical study of the aforesaid model. In the future, this model can be investigated by using an ABC type derivative which has a nonlocal and nonsingular kernel. It would be expected that more dynamic properties may appear for better understanding.

Acknowledgement: The authors K. Shah, T. Abdeljawad, and B. Abdalla thank Prince Sultan University for support through the TAS Research Lab.

Funding Statement: The research was financially supported by Prince Sultan University.

Conflicts of Interest: The authors declare that they have no conflicts of interest to report regarding the present study.

References

1. Rizzardini, G., Saporito, T., Visconti, A. (2018). What is new in infectious diseases: Nipah virus, MERS-CoV and the blueprint list of the World Health Organization. *Le Infezioni in Medicina, 26(3),* 195–198.
2. Susilarini, N. K., Haryanto, E., Praptiningsih, C. Y., Mangiri, A., Kipuw, N. et al. (2018). Estimated incidence of influenza-associated severe acute respiratory infections in Indonesia, 2013–2016. *Influenza and other Respiratory Viruses, 12(1),* 81–87. DOI 10.1111/irv.12496.
3. Zumla, A., David, S. C. H. (2019). Emerging and reemerging infectious diseases: Global overview. *Infectious Disease Clinics, 33(4),* xiii–xix. DOI 10.1016/j.idc.2019.09.001.
4. Farrar, J. J. (1999). Nipah-virus encephalitis–investigation of a new infection. *The Lancet, 354(9186),* 1222–1223. DOI 10.1016/S0140-6736(99)90124-1.
5. Chua, K. B., Bellini, W. J., Rota, P. A., Harcourt, B. H., Tamin, A. et al. (2000). Nipah virus: A recently emergent deadly paramyxovirus. *Science, 288(5470),* 1432–1435. DOI 10.1126/science.288.5470.1432.
6. Nor, M., Gan, C. H., Ong, B. L. (2000). Nipah virus infection of pigs in peninsular Malaysia. *Revue Scientifique et Technique (International Office of Epizootics), 19(1),* 160–165.
7. Clayton, B. A., Middleton, D., Arkinstall, R., Frazer, L., Wang, L. F. et al. (2016). The nature of exposure drives transmission of Nipah viruses from Malaysia and Bangladesh in ferrets. *PLoS Neglected Tropical Diseases, 10(6),* e0004775. DOI 10.1371/journal.pntd.0004775.
8. Bangyao, S., Jia, L., Liang, B., Chen, Q., Liu, D. (2018). Phylogeography, transmission, and viral proteins of Nipah virus. *Virologica Sinica, 33(5),* 385–393. DOI 10.1007/s12250-018-0050-1.
9. Liew, Y., Ibrahim, P., Ong, H., Chong, C., Tan, C. et al. (2022). The immunobiology of Nipah virus. *Microorganisms, 10(6),* 1162. DOI 10.3390/microorganisms10061162.
10. Sinha, D., Sinha, A. (2019). Mathematical model of zoonotic Nipah virus in South-East Asia region. *Acta Scientific Microbiology, 2(9),* 82–89.
11. World Health Organization (2018). List of blueprint priority diseases, R and D Blueprint: World Health Organization.
12. Nita, H. S., Niketa, D. T., Foram, A. T., Moksha, H. S. (2018). Control strategies for Nipah virus. *International Journal of Applied Engineering Research, 13(21),* 15149–15163.
13. Schountz, T. (2014). Immunology of bats and their viruses: Challenges and opportunities. *Viruses, 6(12),* 4880–4901. DOI 10.3390/v6124880.
14. Monath, T. P., Nichols, R., Tussey, L., Scappaticci, K., Pullano, T. G. et al. (2022). Recombinant vesicular stomatitis vaccine against Nipah virus has a favorable safety profile: Model for assessment of live vaccines with neurotropic potential. *PLoS Pathogens, 18(6),* e1010658. DOI 10.1371/journal.ppat.1010658.
15. Wang, Z., Amaya, M., Addetia, A., Dang, H. V., Reggiano, G. et al. (2022). Architecture and antigenicity of the Nipah virus attachment glycoprotein. *Science, 375(6587),* 1373–1378. DOI 10.1126/science.abm5561.
16. Kapur, J. N. (1988). *Mathematical modelling*. New Delhi, India: New Age International.
17. Goh, K. J., Tan, C. T., Chew, N. K., Tan, P. S. K., Kamarulzaman, A. et al. (2000). Clinical features of Nipah virus encephalitis among pig farmers in Malaysia. *New England Journal of Medicine, 342(17),* 1229–1235. DOI 10.1056/NEJM200004273421701.
18. Agarwal, P., Singh, R. (2020). Modelling of transmission dynamics of Nipah virus (NiV): A fractional order approach. *Physica A: Statistical Mechanics and its Applications, 547,* 124243. DOI 10.1016/j.physa.2020.124243.

19. Tan, K. S., Tan, C. T., Goh, K. J. (1999). Epidemiological aspects of Nipah virus infection. *Neurology Asia, 4(1),* 77–81.
20. Cross, R., Woolsey, C., Prasad, A., Borisevich, V., Agans, K. et al. (2022). A recombinant VSV-vectored vaccine rapidly protects nonhuman primates against lethal Nipah virus disease. *Proceedings of the National Academy of Sciences, 119(12),* e2200065119. DOI 10.1073/pnas.2200065119.
21. Chong, H. T., Hossain, M. J., Tan, C. T. (2008). Differences in epidemiologic and clinical features of Nipah virus encephalitis between the Malaysian and Bangladesh outbreaks. *Neurology Asia, 13,* 23–26.
22. Hossain, M. J., Gurley, E. S., Montgomery, J. M., Bell, M., Carroll, D. S. et al. (2008). Clinical presentation of Nipah virus infection in Bangladesh. *Clinical Infectious Diseases, 46(7),* 977–984. DOI 10.1086/529147.
23. Biswas, M. H. A. (2012). Model and control strategy of the deadly Nipah virus (NiV) infections in Bangladesh. *Research and Reviews in Biosciences, 6(12),* 370–377.
24. Atangana, A., Araz, S. I. (2021). New concept in calculus: Piecewise differential and integral operators. *Chaos, Solitons & Fractals, 145,* 110638. DOI 10.1016/j.chaos.2020.110638.
25. Khan, M. A., Atangana, A. (2020). Modeling the dynamics of novel coronavirus (2019-nCov) with fractional derivative. *Alexandria Engineering Journal, 59(4),* 2379–2389. DOI 10.1016/j.aej.2020.02.033.
26. Atangana, A. (2020). Modelling the spread of COVID-19 with new fractal-fractional operators: Can the lockdown save mankind before vaccination? *Chaos, Solitons & Fractals, 136,* 109860. DOI 10.1016/j.chaos.2020.109860.
27. Atangana, A., Qureshi, S. (2019). Modeling attractors of chaotic dynamical systems with fractal-fractional operators. *Chaos, Solitons & Fractals, 123,* 320–337. DOI 10.1016/j.chaos.2019.04.020.
28. Atangana, A., Igret Araz, S. (2021). Modeling and forecasting the spread of COVID-19 with stochastic and deterministic approaches: Africa and Europe. *Advances in Difference Equations, 2021(1),* 1–107. DOI 10.1186/s13662-021-03213-2.
29. Veeresha, P., Ilhan, E., Prakasha, D. G., Baskonus, H. M., Gao, W. (2022). A new numerical investigation of fractional order susceptible-infected-recovered epidemic model of childhood disease. *Alexandria Engineering Journal, 61(2),* 1747–1756. DOI 10.1016/j.aej.2021.07.015.
30. Omame, A., Sene, N., Nometa, I., Nwakanma, C. I., Nwafor, E. U. et al. (2021). Analysis of COVID-19 and comorbidity co-infection model with optimal control. *Optimal Control Applications and Methods, 42(6),* 1568–1590. DOI 10.1002/oca.2748.
31. Yavuz, M., Sene, N. (2020). Stability analysis and numerical computation of the fractional predator-prey model with the harvesting rate. *Fractal and Fractional, 4(3),* 35. DOI 10.3390/fractalfract4030035.
32. Evirgen, F. (2022). Transmission of Nipah virus dynamics under caputo fractional derivative. *Journal of Computational and Applied Mathematics, 418,* 114654.
33. Omede, B. I., Ameh, P. O., Omame, A., Bolaji, B. (2020). Modelling the transmission dynamics of Nipah virus with optimal control. arXiv preprint arXiv:2010.04111.
34. Mondal, M. K., Hanif, M., Biswas, M. H. A. (2017). A mathematical analysis for controlling the spread of Nipah virus infection. *International Journal of Modelling and Simulation, 37(3),* 185–197. DOI 10.1080/02286203.2017.1320820.
35. Biswas, M. H. A., Haque, M. M., Duvvuru, G. (2015). A mathematical model for understanding the spread of Nipah fever epidemic in Bangladesh. *International Conference on Industrial Engineering and Operations Management (IEOM)*, pp. 1–8. Dubai, United Arab Emirates.
36. Diekmann, O., Heesterbeek, J. A. P. (1989). *Mathematical epidemiology of infectious diseases*. New York: Wiley.
37. Shah, K., Abdeljawad, T., Abdalla, B., Abualrub, M. S. (2022). Utilizing fixed point approach to investigate piecewise equations with non-singular type derivative. *AIMS Mathematics, 7(8),* 14614–14630. DOI 10.3934/math.2022804.

38. Zeb, A., Atangana, A., Khan, Z. A., Djillali, S. (2022). A robust study of a piecewise fractional order COVID-19 mathematical model. *Alexandria Engineering Journal, 61(7),* 5649–5665. DOI 10.1016/j.aej.2021.11.039.
39. Kumlin, P. (2004). A note on fixed point theory. In: *Functional analysis lecture*. Chalmers & GU. https://www.studocu.com/sv/document/goteborgs-universitet/functional-analysis/lecture-notes-fixed-point-theory/839173.
40. Khastan, A., Nieto, J. J., Rodríguez-López, R. (2014). Schauder fixed-point theorem in semilinear spaces and its application to fractional differential equations with uncertainty. *Fixed Point Theory and Applications, 2014(1),* 1–14.
41. Kilbas, A. A., Srivastava, H. M., Trujillo, J. J. (2006). *Theory and applications of fractional differential equations*. Amester Dam: Elsevier.
42. Ramos, H. (2019). Formulation and analysis of a class of direct implicit integration methods for special second-order IVPs in predictor-corrector modes. In: *Recent advances in differential equations and applications*, pp. 33–61. New York.